NREL/SR-520-23444 • UC Category: 1260

Application of CIS to High-Efficiency PV Module Fabrication

Annual Technical ProgressReport 1 April 1996 - 31 March 1997

B. Başol, V. Kapur, C. Leidholm,
A. Halani, and G. Norsworthy
International Solar Electric Technology
Inglewood, California

NREL technical monitor: H.S. Ullal

National Renewable Energy Laboratory
1617 Cole Boulevard
Golden, Colorado 80401-3393
A national laboratory of
the U.S. Department of Energy
Managed by Midwest Research Institute
for the U.S. Department of Energy
under Contract No. DE-AC36-83CH10093

Prepared under Subcontract No. ZAF-5-14142-07

August 1997

NOTICE

Available to DOE and DOE contractors from:
Office of Scientific and Technical Information (OSTI)
P.O. Box 62
Oak Ridge, TN 37831
Prices available by calling (423) 576-8401

Available to the public from:
National Technical Information Service (NTIS)
U.S. Department of Commerce
5285 Port Royal Road
Springfield, VA 22161
(703) 487-4650

TABLE OF CONTENTS

LIST OF FIGURES

LIST OF TABLES

1.0 SUMMARY

This is the Phase II Annual Technical Report of the subcontract titled "Application of CIS to High Efficiency PV Module fabrication." The general objectives of the program are the development of a novel, non-vacuum process for CIS film deposition, optimization of the various layers forming the CIS device structure, and fabrication of high efficiency submodules. The specific goals of the project are the development of 13% efficient small area cells and 10% efficient submodules using a novel, low-cost CIS deposition approach.

During this research period, we concentrated our efforts on three different areas of research. Within the National CIS Partnership Program, we participated in the "substrate/Mo interactions" working group and investigated issues such as Na diffusion from the soda-lime glass substrate into the Mo layers and CIS films. It was determined that the Na content within the Mo layers was not a strong function of the nature of the Mo film. However, diffusion through the Mo layers was found to be a function of the Mo film characteristics as well as a very strong function of the CIS growth process. Na was found to be on the grain boundaries both in Mo and CIS layers.

Much of the effort was spent on the development of a low-cost, non-vacuum CIS deposition technique and on the establishment of a pilot facility to process approximately 1 ft^2 size modules. The non-vacuum technique was successfully developed for CIS film growth. Layers prepared using this novel approach were used for solar cell and submodule fabrication. Small area solar cells with active area efficiencies around 13% were demonstrated. Submodules with efficiencies above 8% were also fabricated. The size of the submodules processed is so far limited to about 30 cm^2. 1 ft^2 size module processing will be initiated during the next phase of the program when the pilot line will be de-bugged and challenges faced in the integration process are remedied.

2.0 INTRODUCTION

This is the Phase II Annual Technical Report of a subcontract titled "Application of CIS to High Efficiency PV Module Fabrication". The objective of this program is to develop understanding and solutions for certain issues related to cost-effective production of CIS-based PV modules. The most important task is the development and demonstration of a novel, low-cost method for CIS film growth that does not employ expensive vacuum processing. Other tasks involve module integration and bandgap engineering.

Recent advances made in CIS and related compound solar cell fabrication processes have clearly shown that these materials and device structures can yield power conversion efficiencies greater than 17%. However, despite these very impressive laboratory results, CIS type of solar cells and modules are not yet in production. Part of the reason for this is the fact that the techniques employed in fabricating high efficiency CIS type solar cells are costly and/or they are not well suited for large scale film deposition. ISET's Phase II program is specifically geared towards the development and demonstration of a totally non-vacuum, low cost deposition technique for the growth of CIS absorbers. The vacuum based two-stage processing that was the subject of our Phase I effort has been replaced by this novel non-vacuum approach in the Phase II program. The vacuum based two-stage process was, however, still used in tasks studying some basic phenomena such as substrate/film interactions and bandgap engineering. The approach we selected was to carry out certain initial experiments with the vacuum based processing approach and after understanding the phenomena, to try to apply this knowledge to the new non-vacuum technique.

The specific goals of this 12-month program as listed in our "Statement of Work" and the "Schedule of Deliverables" were: The development of 13% efficient cells of 1 cm^2 area and 10% efficient submodules of 6"x6" area using ISET's novel, low-cost, non-vacuum CIS growth technique.

3.0 TECHNICAL DISCUSSION

In this program ISET's efforts were concentrated on the development of a novel, low-cost non-vacuum deposition process for CIS absorber layers. However, to be able to correlate the data from the "CIS-Mo-substrate interactions" task with our previously obtained results on vacuum based CIS layers, we continued to prepare small size samples by the vacuum-based two-stage process specifically for the task that was formulated to study CIS-Mo-substrate interactions.

Details of ISET's vacuum-based two-stage selenization technique and the device fabrication steps have been previously described [1]. In summary, these baseline processes involved vacuum deposited metallic precursors and vapor phase selenization in H_2Se. Cu-In precursors of various stoichiometries were deposited onto the Mo-coated soda-lime glass substrates at room temperature using the e-beam evaporation method. If needed, gallium addition into the absorber layers was achieved by adding a thin layer of Ga into the Cu-In precursor stack. Selenization of the precursors was carried out in a reactor kept at a temperature of about 450 °C. The reactive atmosphere in the selenization chamber contained a mixture of H_2Se gas and N_2. For device fabrication, CIS films were coated with a thin (600-2000 Å) CdS layer using the solution growth technique. This step was then followed by the deposition of a conductive ZnO window layer using the MOCVD method.

As stated before, tasks involving the development of a novel CIS growth approach did not have any vacuum deposition step. In these tasks, films were grown through a new non-vacuum technique. Device fabrication steps, however, were common to CIS absorbers obtained by both vacuum and non-vacuum approaches.

3.1 CIS-Mo-Substrate Interactions

This task was shared by the "Substrate/Mo Impact" working group that was formed within the National CIS Partnership Team. ISET was a member of this group which also included EPV, Lockheed/Martin, University of Illinois and NREL. The goal was identification and study of the chemical interactions between the glass substrate, Mo layer and the CIS absorber film. Experiments were set up to try to find answers to the questions of the nature of the Na diffusion from the substrate, through the Mo layer and into the CIS absorbers. For each experiment several samples were prepared by the working group members and results on each sample were analyzed with the aim of coming up with a universal explanation for the observed phenomena. In this report we will only present the relevant results obtained from the samples prepared at ISET's laboratory.

Although, glass is commonly distinguished by its high chemical resistance at low temperatures, its reactivity is extensive at temperatures and chemical environments

employed in CIS film growth. The typical composition of a soda-lime glass sheet in weight percentages is 70% SiO_2, 15% Na_2O, and the balance, the oxides of Ca, Al, Mg, Ba and K. The Na-O network in soda-lime glass is known to be reactive and we had previously studied the extensive reactions that are possible between the Na in the glass substrate and the selenization environment [2].

3.1.1. Measurements on sputter deposited Mo layers

Mo is the contact layer that stands between the selenization environment and the soda-lime glass substrate. If no prior processing is done on the surface of the soda-lime glass substrate, Mo can act as the barrier or the conduit for the diffusion of Na from the glass substrate into the growing CIS layer. During this period of research we have carried out experiments to shed light on this very important topic.

ISET has supplied two different Mo films (labeled Mo-135 and Mo-375) to be studied by the "Substrate/Mo impact" working group. The deposition parameters used for the two films and their thicknesses are given in Table I. These films were intentionally deposited in two different sputtering systems and one film (ISET-135) is much thicker than the other as can be seen from Table I.

Table I. Deposition parameters and other properties for two Mo layers prepared at ISET for Na diffusion studies.

Sample	Base Press. (x 10^{-6})	Ar Press. (mTorr)	Sputter Power	Distance (cm)	No. of Scans	Scan Rate (cm/min)	Thickness (μm)
Mo-135	5	8	13	4	4	2	2.3
Mo-375	1.5	6	25	4	2	16	0.4

The Mo layers were first analyzed by SEM and XRD to see if there were any obvious differences between them in terms of their microstructure and preferred crystal orientation. Cross sectional SEM studies showed that both layers had columnar structures with filamentary grains of 0.05-0.1 micron size. Since the Mo films were grown by passing the substrates multiple times in front of a Mo target, this layered structure was clearly seen in the cross sectional SEMs.

As-deposited Mo layers were analyzed by SIMS to determine their Na content. They were then subjected to a heat treatment step under vacuum at around 450 °C. Other pieces of the same samples were exposed to a H_2Se+N_2 atmosphere for 30 minutes at 450 °C. All the samples were analyzed by SEM, XRD and SIMS.

The XRD analysis results for the as-deposited and selenized Mo layers are given in Table II. The data has been normalized to the maximum intensity. As can be seen from this data, the layers have (110) preferred orientation. For the as-deposited films, there does not seem to be any correlation between the type of Mo and the preferred crystalline orientation. After the selenization step, peak intensities seem to change, but not in a consistent manner to suggest a pattern. SEM cross sectional studies did not indicate any obvious changes in the microstructure of the films as a result of the selenization step. However, after selenization, parts of Mo-375 Mo film were destroyed. It could not be determined whether this was purely a physical detachment of the film from its substrate. It was, however, clear that selenization affected this Mo layer much more than it affected Mo-135.

Table II XRD Mo peak intensities for the two samples before and after the selenization step.

Sample	Max Counts	(110)	(211)	(220)	(321)
Mo-135	513867	100	5.5	3.61	2.59
Selenized		100	4.72	4.06	
Mo-375	326333	100	4.92	3.55	2.57
Selenized		100	16.3	7.65	

The XRD data obtained at NREL for selenized Mo-135 and Mo-375 layers are shown in Fig.1. Mo and Mo-Se peaks are labeled in this data. We did not detect any Mo-Se related

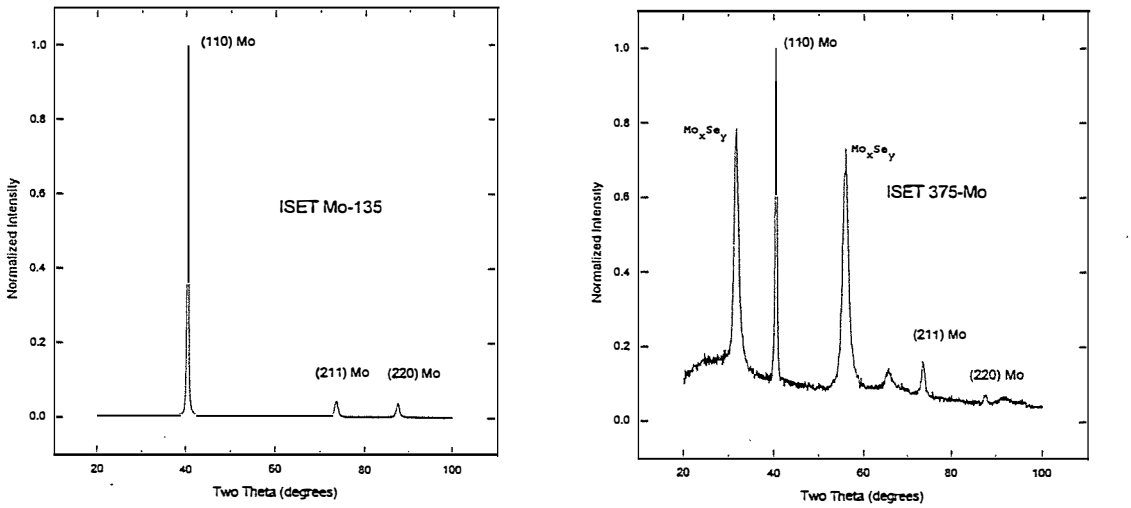

Fig. 1 XRD data obtained from two Mo layers after their selenization in H_2Se atmosphere: a) Mo-135, b) Mo-375.

peaks in ISET-135, although we knew there was a thin layer of selenide at its surface which was detected by SIMS and Auger measurements. The rather large selenide peaks of sample Mo-375 are thought to be associated with Mo_3Se_4 and Mo_9Se_{11} phases. Once again this data indicated the extensive interaction of the selenization atmosphere with one of the two Mo layers studied. The SIMS profiles taken at U. of Illinois for the two ISET Mo films after the vacuum annealing step are given in Fig. 2. All profiles have had their signals devided by the Mo count rate so that changes in machine operating conditions were corrected for. The general conclusions from this data are as follows:

i) There is no effect of annealing on the oxygen profile for a 450 °C, 20 minute anneal in vacuum.

ii) There is a quantitative increase in Na signal but no qualitative change in Na profile upon annealing. More Na comes into the Mo layer as a result of the annealing step. However, the basic shape of the profile does not change. The suggestion is that the Na diffusion takes place along the grain boundaries and it is fast. Therefore, we do not see an actual diffusion profile, but we observe a constant increase of Na throughout the Mo layer.

iii) One other interesting observation from the data of Fig. 2 is the fact that the Na level in both Mo layers is roughly identical despite the fact that the deposition conditions and the selenization character of the two layers were very different as we have seen from previous data.

iv) Na signal and O signal track each other, suggesting that Na is in the form of an oxide in the Mo layer. It most possibly resides on the grain boundaries. If this is the case, the Na level observed in the SIMS profile is actually an indication of the Mo grain boundary area in each film. It should be noted that the peaks in the Na and O signals coincide with the interfaces between the sub-layers of the multi-layered Mo films analyzed in this study.

SIMS profiles obtained from the samples that were selenized at 450 °C for 30 minutes in H_2Se atmosphere are given in the data of Fig. 3. As can be seen from this data selenization affected the samples just as the annealing did. In other words, the Na level was increased uniformly throughout the samples as a result of the selenization step. There is no diffusion profile and there is a Se signal which is high near the surface and it gets lower in the bulk of the Mo layer. this shows the surface Mo-Se layer formed as a result of the selenization step.

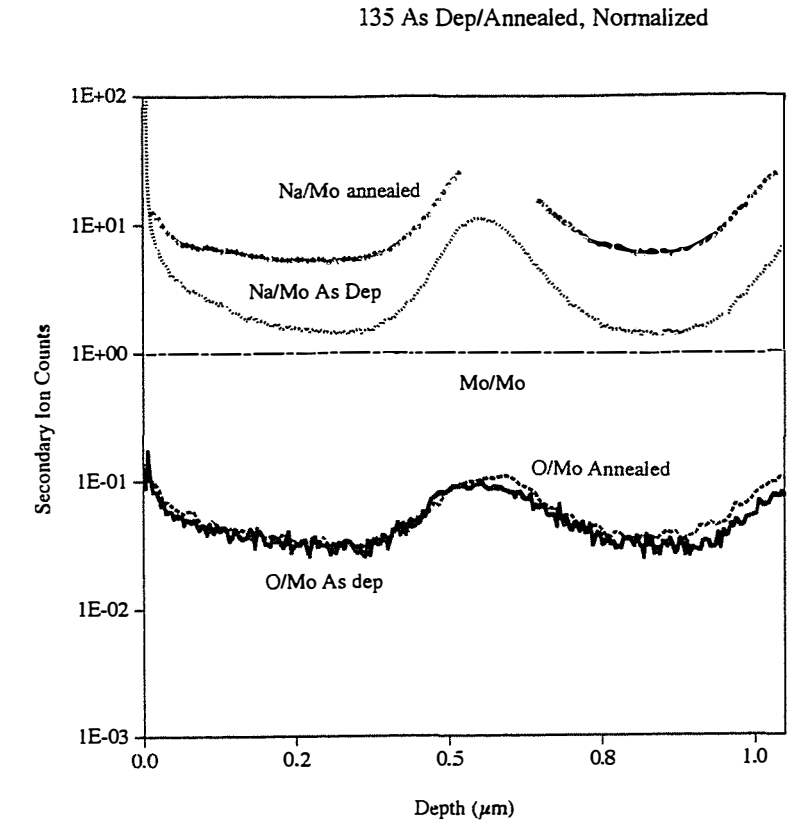

Fig. 2 SIMS profiles taken from the two Mo layers indicating the affects of a 450 °C, 20 minutes heat treatment in vacuum.

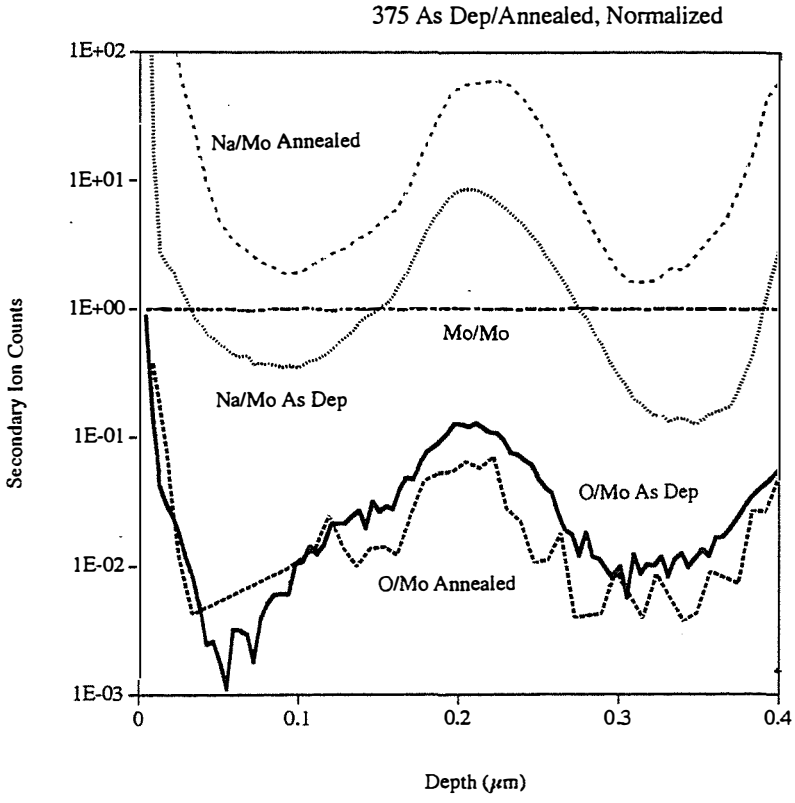

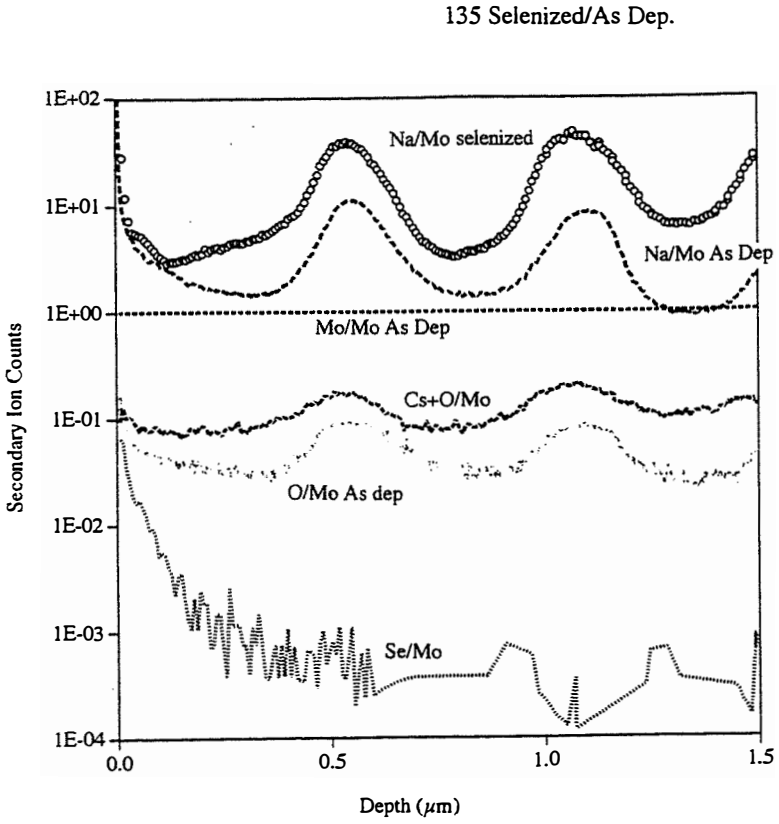

Fig. 3 SIMS profiles obtained from the two Mo layers that were selenized in H_2Se atmosphere at 450 °C for 30 minutes.

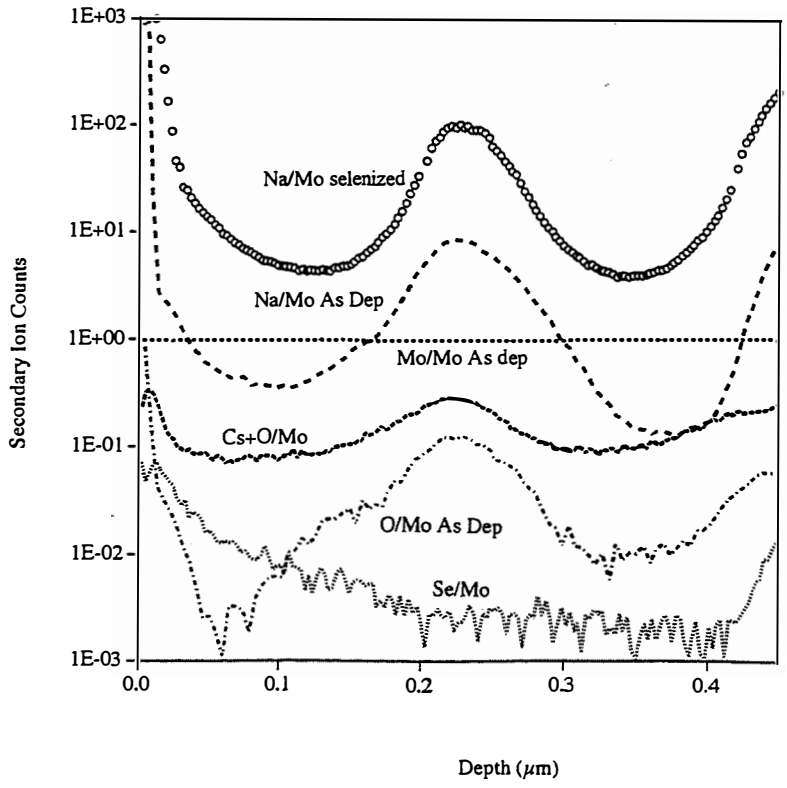

3.1.2. Measurements on CIS layers

After studying Na diffusion into the Mo layers, we deposited CIS films on the glass/Mo structures by the two-stage selenization approach and carried out analysis to determine the Na content of these CIS layers. The selenization step consisted of a 30 minute reaction in H_2Se+N_2 atmosphere at 450 °C. Therefore, temperatures and times employed during selenization were close to the temperatures and times used for the annealing experiments of the last section. SIMS profiles were taken at NREL through both the CIS and the Mo layers using Cs+ primary ions, 10kV, with nominal impact energy of 5.5 kV. Profiles were normalized to the 82Se+Cs signal so that direct comparison between levels could be made. The depths were scaled for the difference in sputter rate between the Mo and CIS layers. The results are shown in Figs. 4a and 4b.

It is obvious from the data of Figs. 4a and 4b that the Na content of the CIS film deposited on Mo-375 is about 3-4 times higher than that of the one grown on Mo-135. This result suggests that the diffusion of Na through the thin Mo layer is higher. There is also a high level of Na near the Mo/CIS interface in both samples. This level is probably saturated and the actual Na amount is much higher than is suggested by the profiles of Fig. 4. High Na content near the Mo/CIS interfaces and the decreased Na concentration in the bulk of the CIS layers may appear like Na diffusion profiles . However, we believe that this profile is an artifact of the microstructure of the CIS layers. Near the Mo interface, CIS layers are expected to be small grained. Then the grains are expected to grow as one goes into the bulk of the layers. If Na resides primarily on the grain boundaries, then it is conceivable that what we are observing in the Na SIMS profiles is actually the effective grain boundary areas in various portions of the films. SEM studies are in progress to clarify this point.

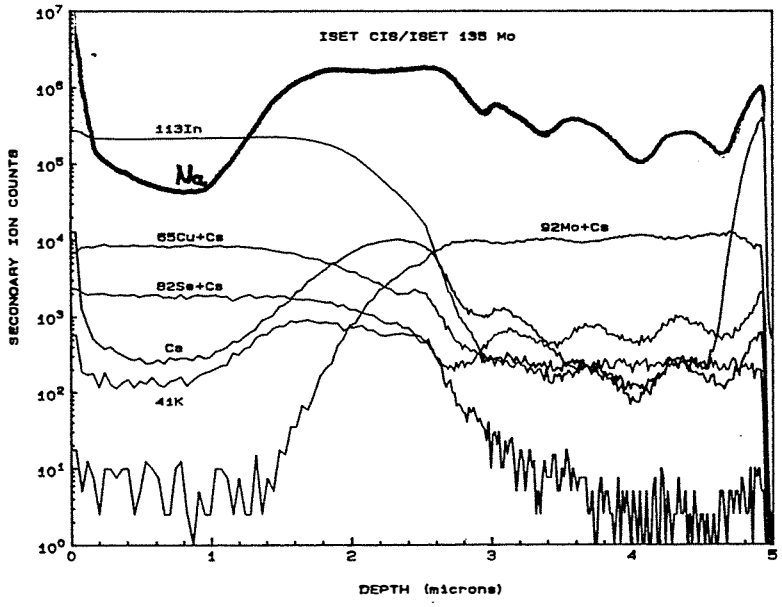

Fig. 4a SIMS profile taken through a CIS layer grown by two-stage selenization approach on Mo-135 sample.

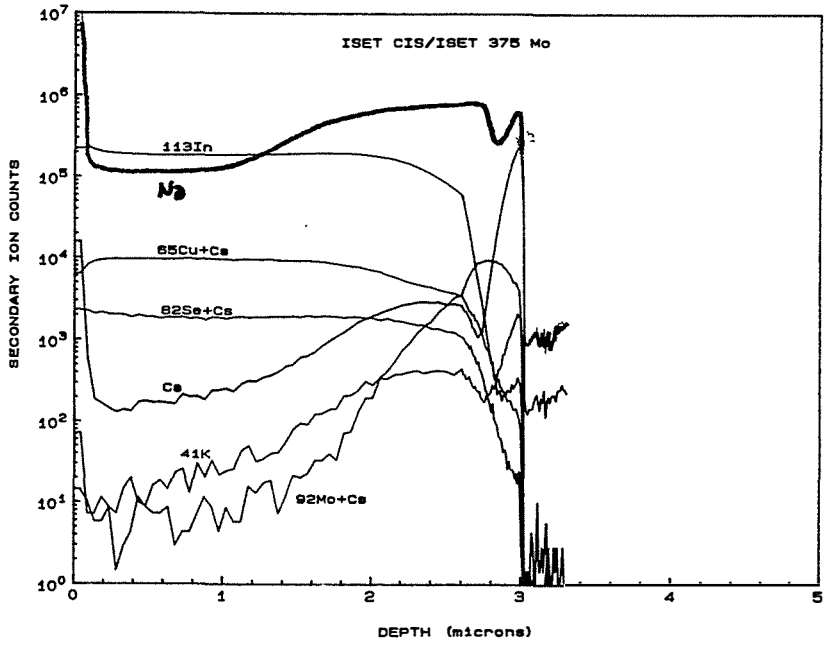

Fig. 4b SIMS profile taken through a CIS layer grown by two-stage selenization approach on Mo-375 sample.

In conclusion, Na diffusion studies made on samples with glass/Mo and glass/Mo/CIS structures indicated that:

I) Na content of the Mo layers was approximately the same for two different films with different characters in terms of their thickness and resistivity.

ii) Despite the fact that the Na content was the same in both layers, Na diffusion through these layers were very different, diffusion being faster through the thinner Mo film.

iii) Na primarily resides on the grain boundaries and is associated with oxygen especially when it is in Mo layers.

iv) When different selenization techniques were studied (not reported here) Na content in the CIS films was found to be a very strong function of the selenization method. H_2Se selenization promoted the highest degree of Na diffusion into the CIS layers. This result suggested that the most important factor determining Na diffusion into CIS was the process used in growing the CIS layers rather than the nature of the Mo layer.

3.2 Novel CIS Deposition Technique

As stated before, CIS and related Group I-III-VI compound absorbers have been used in thin film solar cell structures and devices with over 17% conversion efficiency have been demonstrated. A review of the literature shows that high efficiency CIS cells have so far been fabricated on layers grown by the vacuum co-evaporation technique or by various versions of the two-stage selenization method employing evaporated or sputter deposited precursor films. Evaporation techniques are difficult to scale up because of film uniformity and material utilization considerations. Sputtering techniques are better suited for large area deposition, however, they require expensive vacuum equipment and sputtering targets. Materials utilization in sputtering targets is also poor. Therefore, a low cost, non-vacuum technique with the capability of processing large area substrates would be very attractive for the growth of CIS layers for photovoltaic applications. In this report, we present data on a new non-vacuum deposition technique developed at ISET.

Soda-lime glass substrates were used in this work. Mo contact layers were deposited on the soda-lime glass substrates by D.C. magnetron sputtering. CIS films were grown on the Mo surface by the non-vacuum technique. Solar cell fabrication steps included deposition of a thin CdS layer by the commonly used chemical bath deposition approach. A ZnO layer was then deposited on the CdS surface using a MOCVD method. Solar cells of 0.09-1.00 cm^2 area were defined on the substrates using photolithographic techniques. Both films and devices were characterized to understand the nature of the material grown by the non-vacuum approach. In addition to solar cell fabrication, some work was also done on sub-module processing. The module integration approach was the same as the technique used on vacuum based devices. The Mo scribing was done by laser. The two scribes following CIS deposition were done mechanically.

3.2.1 Devices fabricated on non-vacuum CIS layers

The solar cells fabricated on CIS layers obtained by ISET's non-vacuum technique (from now on referred to as the "non-vacuum films/cells") initially yielded efficiencies in the 8-10% range, clearly demonstrating the potential of this low cost process. The illuminated I-V characteristics and the relative spectral response of such an early device is shown in Fig. 5. This cell had a respectable V_{oc} and a good fill factor value. The J_{sc} value, however, was rather low at 32.78 mA/cm^2. An in-depth analysis of the device was then carried out to determine its parameters, the carrier density of the CIS film and the photocurrent loss mechanisms causing the observed low J_{sc} value. The results of this analysis is shown in Table III under the column labeled "10% cell". A review of the device parameters, the carrier density of the film, and the photocurrent losses due to the window layer absorption, reflection and deep penetrating photons, indicated that the early devices fabricated on films grown by the non-vacuum process were very much comparable with the CIS cells

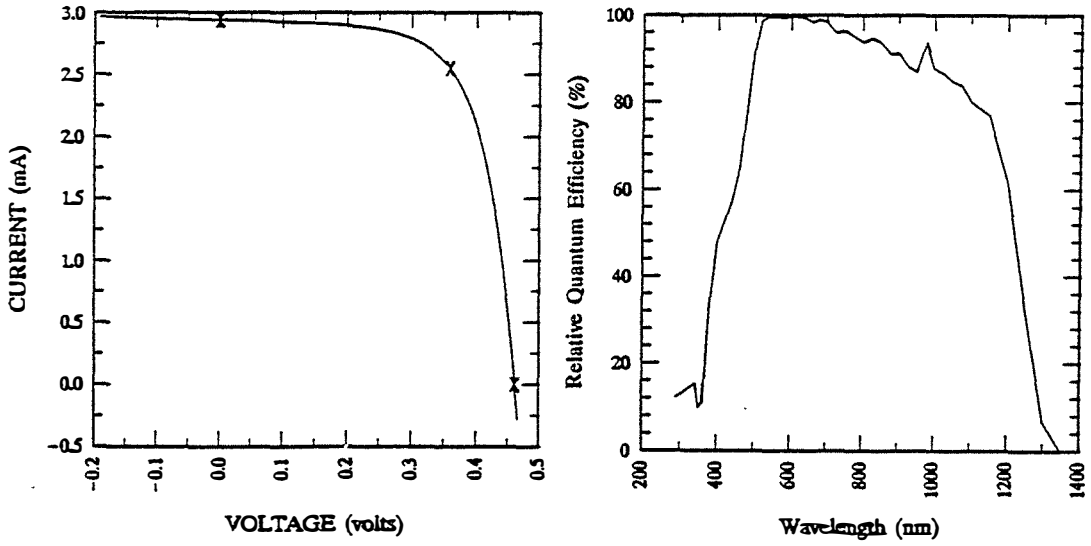

Fig. 5 Light I-V characteristics and relative quantum efficiency of a 0.09 cm^2 device fabricated on non-vacuum CIS film. V_{oc}=0.4616 V, J_{sc}=32.78 mA/cm^2,FF=67.51%, η=10.2%.

fabricated at ISET on evaporated and selenized absorber layers. The only notable difference, however, was the rather large unidentified photocurrent loss of about 7 mA/cm^2, which brought down the quantum efficiency curve uniformly across the whole spectrum of the measured response. SEM, EBIC and EDS studies were then initiated to understand this phenomenon.

TABLE III. Device parameters, carrier densities and photocurrent loss mechanism analysis results for the two cells fabricated on non-vacuum CIS layers.

Parameters	10.2% cell		12.4% cell	
	Light	Dark	Light	Dark
Shunt r (Ω-cm^2)	700	1100	1300	3400
Series R (Ω-cm^2)	0.2	0.2	0.3	0.5
Diode Factor, A	1.9	2.0	1.6	1.55
p (x 10^{16} cm^{-3})	2.7		1	
J_{sc} Losses (mA/cm^2)				
reflection	3		4	
window loss	2		2	
deep penetration	3.5		3.3	
unidentified	7		1	

Figure 6 shows a surface EBIC image taken from the device of Fig. 5. Clearly, there was a high density of "low-response" regions in this cell, which appear as dark spots in the EBIC image. The dark regions constitute about 20% of the total device area shown in Fig. 6. If we assume that these areas do not contribute at all to photocurrent collection, this clearly explains the origin of the unidentified, wavelength independent current loss of 7 mA/cm^2 observed in the data of Table III.

Most of the small-size low-response areas in Fig. 6 are round in shape with diameters ranging from 5μm to 30 μm. A closer look at the larger (up to about 150 μm in one dimension) low-response regions revealed that these areas were created by convergence of two or more small-size low-response areas, and that there was almost always a large protruding dome-like surface feature close to the center of each low-response area. A high magnification SEM of a 100 μm size low-response area is shown in Fig. 7.

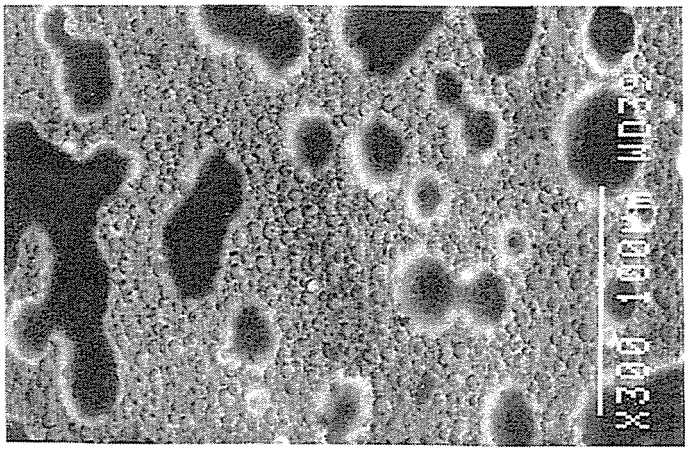

Fig. 6 EBIC surface image of the cell of Fig. 5.

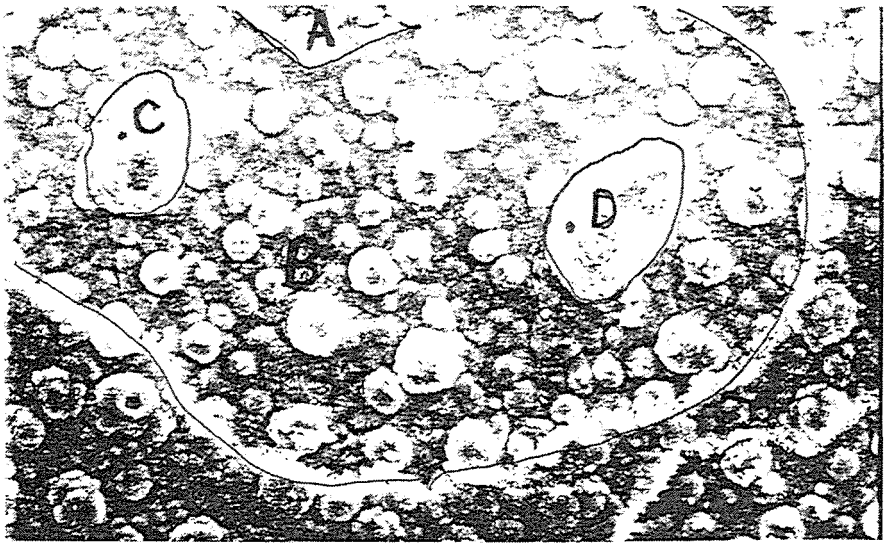

Fig. 7 SEM of a low-response region showing the large surface features (C and D). EDS data was taken from locations A,B,C and D. The scale bar corresponds to 10 μm.

The large surface features labeled as C and D are clearly seen in this micrograph. EDS analysis made at the locations indicated on this figure showed that the active device region (A) contained both Zn and CIS, whereas, the spots within the low response region (B,C,D) contained only CIS. The chemical composition of the CIS material at points B,C and D were all the same. Therefore, it was concluded that the low response areas were caused by physical detachment of the CdS/ZnO window layer around the region where the dome-like surface features were present, and that the large surface features at C and D did not result from a compositional non-uniformity, such as excess Cu, in the CIS films obtained by the non-vacuum method. Cross sectional SEM was then used to investigate the nature of the dome-like features.

The micrograph of Fig. 8 shows the cross sectional SEM taken of one of the dome-like features of the sample of Fig. 5. This data suggested that the dome-like features resulted from the presence of near-spherical voids within the CIS layer. It was further observed that a 3 μm size void could effect an area of approximately 10 μm diameter in size, and that some of the domes (not shown in Fig. 8) lacked the ZnO layer on top of them. Having determined the origin of the photogenerated current loss and the rough surface structure of the CIS layer giving rise to that loss mechanism, efforts were concentrated on the improvement of the morphology of CIS films grown by the non-vacuum technique. The stoichiometric uniformity and electronic quality of these films would clearly be adequate for the fabrication of higher efficiency devices once their morphology is improved.

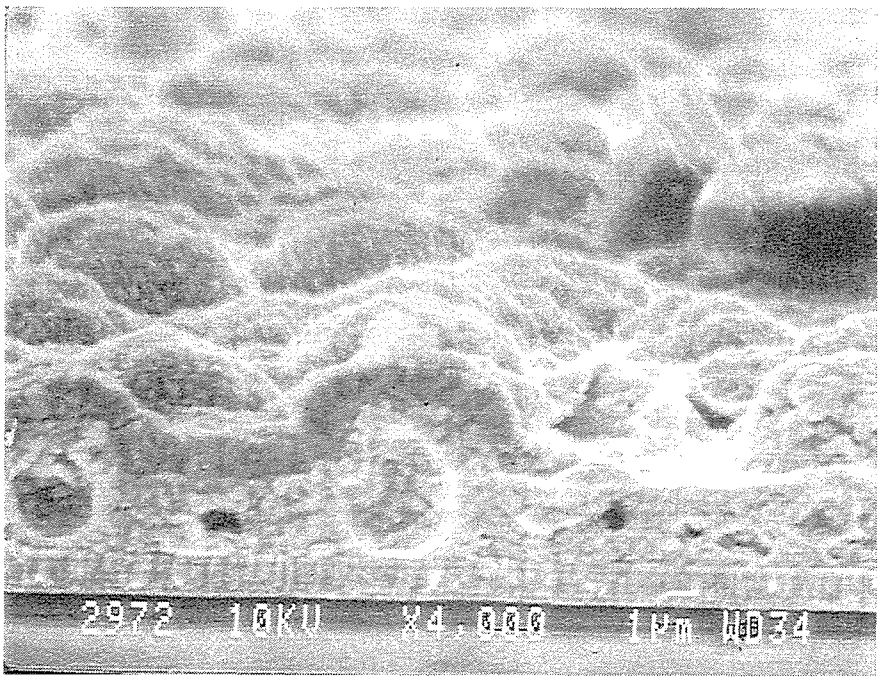

Fig. 8 Cross sectional SEM of the sample of Fig. 5. The top 1.5μm layer is ZnO. The CIS layer is about 3 μm thick. The dome-like features have spherical voids under them as can be seen from this data.

The cross sectional SEM of Fig. 9 shows the morphology and grain structure of the new generation of films prepared by ISET's non-vacuum technique. Although there are still small voids present near the CIS/Mo interface, the surfaces of these layers are smoother than those of the early films discussed before. The grain structure observed in Fig. 9 is also improved. Well formed columnar grains of >1 μm size can be seen in this micrograph.

The illuminated I-V characteristics and the relative quantum efficiency of a device fabricated on the film of Fig. 9 are shown in Fig. 10. It should be noted that we published this data in our previous annual report, however, in depth analysis of the films and devices have been carried out during this period. The short circuit current density of this 0.09 cm^2 area device is over 38 mA/cm^2 and the total area efficiency is 12.4%. The calculated active area efficiency is 13.3%. The analysis results of the cell of Fig. 10 are tabulated in Table III, under the column labeled "12.4% cell". This improved device had lower

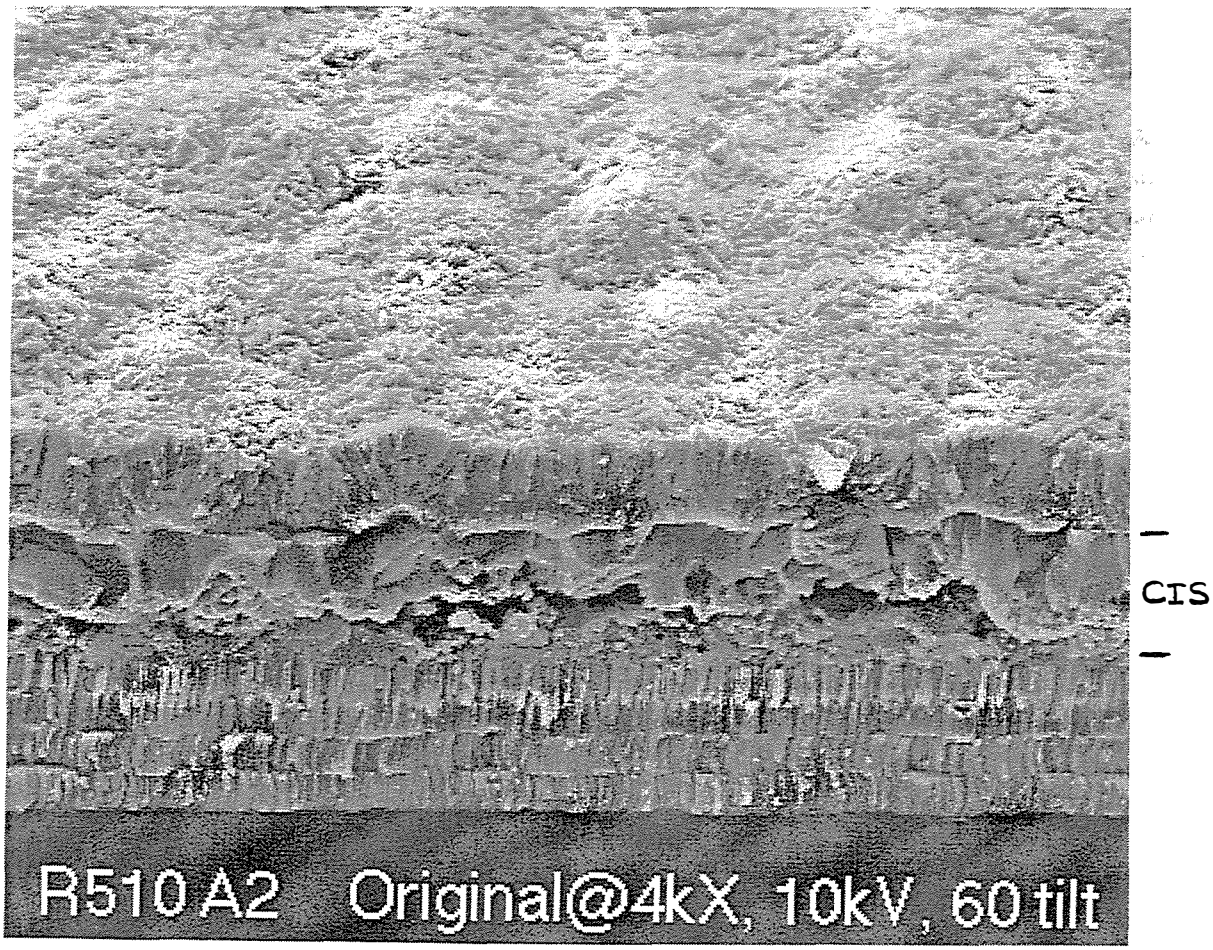

Fig. 9. Cross sectional SEM taken from the improved device demonstrating lower void density and better film morphology. The scale bar corresponds to 1.0 µm.

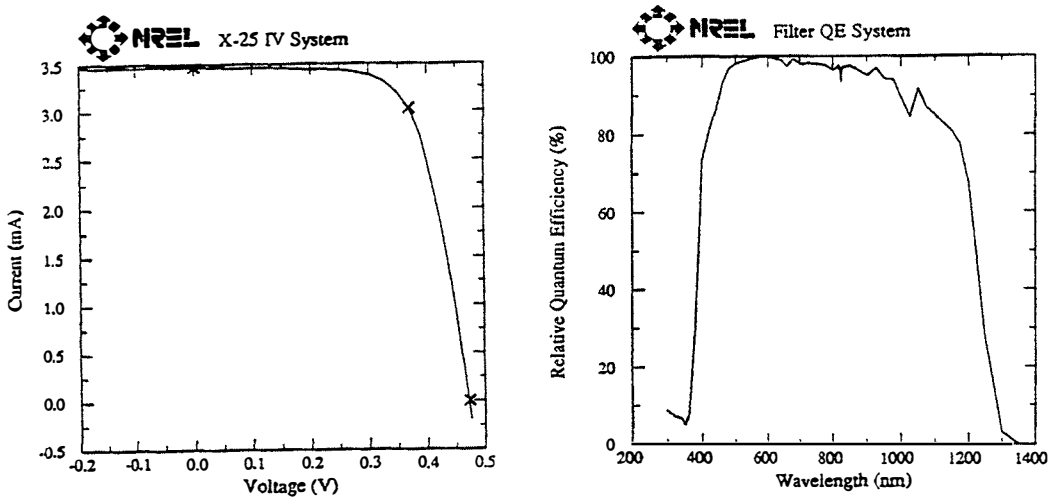

Fig. 10. Light I-V characteristics and the relative Q.E. of a 0.09 cm^2 area cell fabricated on the sample of Fig. 9. V_{oc}=0.4728 V, J_{sc} =38.46 mA/cm^2, FF=67.97% and η=12.4%.

diode factor values and the unidentified current loss mechanism disappeared, as expected. When the quantum efficiency data of Fig. 5 and Fig. 10 are compared, it can be seen that the improved device has better long-wavelength response which is reflected in the smaller loss due to deep penetrating photons as indicated in Table III.

It should be noted that ISET has fabricated several 12% efficient devices during this period of research. The average efficiency, however, has been in the 9-10% range. We identified the film morphology to be the limiting factor in these range of device efficiencies. Higher efficiency devices by the non-vacuum technique will be possible when Ga and/or S addition into the absorbers is achieved. During this research period decision was made to place emphasis on the improvement of yields of the process and the setting up a pilot line that can process 13"x13" size substrates. Much of the effort, therefore, was put into design of the process equipment, building of the equipment and debugging of the process on the pilot line. Work on submodules was continued on small scale to demonstrate 6-8% efficient devices. A 8.17 % submodule with about 25 cm^2 area was submitted during the previous research period. During this period, although we just completed the building of our pilot line, we have not yet produced 1 ft^2 size modules employing it. Debugging process is expected to be completed soon so that such modules can be prepared. In the next section of this annual report we will present information about our efforts to design and construct the pilot line based on our non-vacuum CIS deposition process.

3.2.2 Na doping studies

Electrical doping effects of Na on CIS layers are well recognized. During this research period we carried out experiments to evaluate the feasibility of Na doping of absorber

layers using our non-vacuum process. These experiments involved introducing Na into the growing film and deposition of a Na barrier on the soda-lime glass substrates.
First two Mo substrates were prepared, one incorporating a SiO_2 diffusion barrier (Mo-362-2) and other without (Mo-362-1). The SiO_2 was RF sputtered from a 6" round quartz target in pure Ar at a pressure near 15 mTorr to a thickness of 0.20 µm. Mo was DC sputtered at low pressure (2 mTorr) on both substrates simultaneously, achieving 0.51 µm.

A small sample of each was reserved un-coated for evaluation of the Mo reactivity. Each of the Mo-coated samples was then selenized in an H_2Se atmosphere near 400 °C. The SiO_2 coated sample had a blue reflection, and was highly reflective. The sheet resistance of this sample was not noticeably affected by the selenization step. The sample without the SiO_2 barrier had a typical cloudy surface where a reaction occurred.The sheet resistance of this surface layer was approximately 5 times greater than before the selenization step. From this it was obvious that the SiO_2 barrier plays a significant role in the Mo surface reactivity.

An experiment was designed to better quantify the Na concentration obtained by diffusion from the substrate. Two Mo runs were performed (0.5 µm), each on two SL glass samples, one with a 0.2 µm SiO_2 barrier (771,774) and one without (770,773). The CIS film was deliberately doped with different levels of Na. Two levels of Na were used for this experiment, the heavily doped samples (770, 771) having ~35 times more Na than the low doped samples (773, 774).

In parallel with that experiment, another experiment was devised to investigate the effects of Mo deposition pressure (and thus internal film stress) on films and devices. It has been suggested that Na diffusion is restricted more by Mo films with compressive stress (low pressure) than with tensile stress (high pressure). Therefore, two more Mo runs were performed (0.5 µm), each on two SL glass samples, one with a SiO_2 barrier (777,779) and one without (776,778). One run was performed at low pressure (2 mTorr, samples 776 & 777), the other at a relatively high pressure (11 mTorr, samples 778 & 779). The Mo-coated samples were then coated with a heavily Na doped CIS film.

One final experiment was conducted to investigate the combination of low Na doping and high pressure Mo (11 mTorr) with a SiO_2 barrier, sample 782.

None of the samples had significant adhesion problems and were processed for devices. CdS was deposited by the solution coating method to ~ 1000Å, and ZnO by MOCVD to ~ 2 µm. During ZnO deposition, one sample, 774, peeled from the Mo and was unable to be processed further. The other samples were processed and an array of 16, 0.09 cm^2 devices were made on the 1" x 1" samples. Table IV shows the results of these measurements.

Table IV. Solar cell parameters obtained using CIS absorbers grown on various types of Mo layers and different degrees of Na doping.

Sample Number	Mo Press. (mTorr)	SiO_2?	Na conc.	V_{oc}^* (mV)	J_{sc}^* (mA/cm^2)	FF* (%)	Eff.* (%)
770	5	N	High	70	18	26	0.5
771	5	Y	High	340	28	54	5.1
773	5	N	Low	300	28	49	4.0
774	5	Y	Low	-	-	-	-
776	2	N	High	130	16	27	0.9
777	2	Y	High	260	29	55	6.0
778	11	N	High	160	20	30	1.3
779	11	Y	High	360	28	52	5.6
782	11	Y	Low	400	33	65	9.0

* At least 10 devices on each sample were measured. Values shown are averaged over the total measurements for each sample.

Some of the observations from this experiment were as follows: The SiO_2 barrier gave more uniform distribution of device performance over the entire sample area, and control over Na concentration in the CIS films. Lower Na doping gave overall better devices suggesting that there is an upper limit to the amount of Na that can be included in the film before the electrical characteristics deteriorate. We also observed that low pressure deposited Mo films caused film mechanical integrity problems.

3.3 Setting Up a Pilot Line

During this research period, ISET has begun to set up a pilot line for the demonstration of its thin-film non-vacuum CIS module technology. It is estimated that the planned pilot line will operate at a 50 kW/yr/shift capacity assuming 7% module efficiency and 70% process yield. The pilot line occupies approximately 2000 ft^2 of floor space and consists of ten (10) primary processes including Mo deposition, Mo patterning, materials preparation, film application, annealing processes, chemical bath CdS, MOCVD ZnO, mechanical scribing and module lamination. The pilot line is being designed to initially accommodate 13" x 13" substrates. However, much of the pilot line has been designed to easily accommodate 26" x 13", allowing 2' x 1' modules to be produced.

The Mo deposition process consists of two steps, glass cleaning and sputtering. The glass cleaning is performed in an industrial stainless steel dishwasher equipped with a deionized water rinse option. The washer can hold eighteen (18) substrates per 35 minute run.

The Mo sputtering is accomplished with an MRC 603, loadlock-equipped vertical sputtering machine with three DC magnetron cathodes, each 15" x 5" in area. It is capable of depositing a uniform (±5%), high quality Mo layer on 13" x 13" substrates. By simple modifications, the MRC 603 can sputter all three cathodes simultaneously, producing approximately 10,000 substrates per shift, per year.

Molybdenum patterning involves several processes, including photo resist application, exposure, developing, etching and resist stripping. Another means of Mo patterning used in PV manufacturing is laser scribing. This process does not involve any photolithography or etching processes, and thus is much simpler. However, because of the capital cost of the necessary laser equipment, this process is also much more expensive. For this reason, ISET is using the photolithography-based processes for pattern delineation.

A dry negative-resist process which is widely employed in the circuit board industry is used because of its simplicity compared with spin-on or sprayed resist processes. The dry photo resist film is 1.3 mils thick and is sensitive to UV light. Unlike many resist materials, dry resist is considered to be environmentally benign. This eliminates costly waste disposal, commonly associated with photolithography processes. The dry resist film is applied with a heated pinch-roller, which lays the resist material on the substrate as it passes through two spring-loaded rollers. By adjusting the roller tension, temperature and roll-speed, a uniform, bubble free and well adhering substrate is produced. The resist laminator can accommodate substrates up to 16" wide and virtually any length, as it is an in-line process. This process is relatively fast.

The exposure unit incorporates two UV-rich sodium lamps, producing a high intensity source for exposure. It is capable of exposing 24" x 24", but the uniformity on this size substrate has not yet been studied. However, the exposure uniformity across a 13" x 13" substrate was found to be very good. A flexible poly shadow mask is used for pattern transfer, and is registered by vacuum sealing it to the substrate inside a framed cavity. The current mask pattern uses fifty-two (52), four (4) to six (6) mil lines spaced approximately 6 mm apart.

Developing of the photo resist is done in a vented wet line using Sodium Bicarbonate (Na_2CO_3). The substrates are rinsed and dried before proceeding to the etch line.

Mo etching and stripping is performed in a six-tank vented wet line. Mo etching can be done using many different chemicals and solutions. The one chosen by ISET is Ferric Chloride ($FeCl_3$), because of its low cost, availability and widespread usage and acceptance by other industries such as the PC board industry. The etchant is maintained

at 30°C and the substrates are dipped for approximately 1 minute. The substrates are then spray-rinsed in water and then stripped with a Sodium Hydroxide solution. The resist's chemical makeup causes it to lift-off, rather than dissolve. This leaves resist debris in the strip tank which is overflow-filtered and discarded. The resist material used is environmentally benign, eliminating the need for costly hazardous waste disposal, common in many photo resist processes. A water rinse followed be a deionized water rinse is performed and the substrates are dried with an air knife.

The absorber films are applied to the desired thickness on the substrates and they are subjected to annealing steps at around 400-450°C to achieve the necessary optical and electrical properties.

Cadmium sulfide (CdS) is used as the n-type heterojunction partner. The chemical bath method employed in ISET's research has been scaled up for use in the module production. The chemical bath deposition system was designed to deposit cadmium sulfide on 13" by 13" by 1/8" thick substrates. The major issues in the design of the system were the surface to volume ratio of the system, the heating rate and the solution flow pattern.

The CIS/CdS layers are mechanically scribed to open vias for the ZnO to reach the Mo back contact, to complete the monolithic integration. This is done by mechanical scribing. ISET has a 12" x 12" precision x-y table capable of scribing 11" x 11" substrates. It is currently powered by single stack stepper motors and controlled by a plug-in motion control board in a PC. A larger 26" x 26" precision x-y table has been purchased and will be implemented soon. This new table will be capable of scribing 25" x 25" substrates and will be powered by high-powered servo motors for quick acceleration and deceleration. The larger table will be controlled by the same PC and plug-in board, with a slight modification to the controlling software. The mechanical scribe used is a precision-spring-loaded diamond-tipped stylus, mounted on a z-axis stage. The stylus is monitored by a CCD camera located just above the substrate, allowing the system operator to view the operation on a 10" monitor. The throughput of this scriber is currently limited. However, by incorporating two or three stylus simultaneously, this throughput can be greatly improved.

ZnO deposition is performed in a 14" x 14" MOCVD reactor. The reactor utilizes diethylzinc and water reacting at ~175°C to form the ZnO film. The material is doped using a controlled flow of diborane (B_2H_6), supplying boron to the film. A 30 minute run yields a 2.5 µm film with a sheet resistance of ~5 Ω/□. The throughput of this system is approximately 4000 substrates per year. The MOCVD reactor system is a relatively simple system, and a larger system has been designed. When higher throughput is needed, it can be quickly built and implemented.

Module lamination is performed in a 53" x 18" vacuum cavity laminator. The process seals the surface of the CIS module under tempered glass using an EVA inter-layer. The

sandwich structure is heated in vacuum to remove any air bubbles. As the temperature is increased, a silicone bladder is lowered onto the sandwich which presses any remaining air pockets out of the EVA material. The EVA is then cured at 150°C for about 10 minutes.

3.3.1. Pilot line computer control and data acquisition system

There are numerous ways to execute control of an integrated system. Systems may consist of one control loop or one thousand. For relatively simple systems, independent controllers for each separate function may be satisfactory, if little or no inter communication is required. As system complexity increases, smart controllers must be incorporated, which are able to make decisions based on input received from sensors or independent controllers. This type of system is often executed with the use of Programmable Logic Controllers (PLC's). However, PLC's are relatively limited to single-system control. For control of multiple systems, a CPU is often incorporated to oversee the entire collection of systems, each of which may be controlled by its own CPU, PLC's or independently-controlled sub-systems. This is known as a distributed system, since the control of each sub system is relinquished to its own controllers. The central CPU in this case holds a supervisorial position, overseeing general sub-system operation, but not individual control algorithms such as heating or gas flow control. This type of system is very common in large manufacturing schemes. In smaller multi-system schemes, where system complexity renders independent controllers insufficient, but which are not large enough to warrant distributed control, a central CPU is capable of controlling each sub system itself. This allows a small multi-system setup, where deviations from normal operation can be important, to be scrutinized by the central CPU.

ISET's pilot facility consists of systems capable of producing thin film CIS modules, including Mo sputtering, photolithography, wet line for cleaning and etching, CdS deposition, CIS formation, ZnO deposition, scribing, lamination and IV measurement. Eventually, all of these systems will be connected to a central CPU and the distributed control scheme will be used to control and monitor the overall production. In the initial stages, computer control is used to control only the reaction furnaces, in which the CIS absorber material is produced. Because of the "pilot" stage that ISET is currently in, these systems must be as versatile as possible, to allow for easy modifications to both hardware and control equipment configurations. Moreover, the experience that is gained during this initial pilot-line stage is extremely valuable and is largely dependant on the data that can be collected. Therefore, a central CPU has been chosen to control these subsystems, due to its flexibility and its capability to monitor and accumulate large amounts of data. As the pilot line progresses, each of the sub systems mentioned above will be included in the overall control scheme, and monitored by the central CPU in a distributed fashion.

A computer control system generally consists of both hardware to interface between the CPU and the controlled system, and software to control the actions of the hardware.

ISET has chosen as its software, LabWindows/CVI, a C-language-based environment for Windows programming which offers greater flexibility and capability to the software engineer. The development environment is designed for use with GPIB, VXI, and RS-232 devices as well as plug-in data acquisition (DAQ) boards. LabWindows/CVI can be run on Windows 3.1, Windows 95, Windows NT and SUN Solaris operating systems. Moreover, the development tools are compatible with MS Visual C++, Borland C++, Symantec and WATCOM environments. And the user interface tools are very versatile, allowing clear and intuitive interfaces to be easily designed and executed.

IBM-compatible personal computers currently are the most widely accepted CPU in laboratory and industrial applications. ISET's system is implemented on a Pentium-powered PC, with the keyboard and monitor located on the facility floor for easy access by manufacturing personnel. For safety and data reliability, the system is powered by an uninterruptable power supply (UPS) capable of running the control system for 20 minutes at full load in case of a power failure. In case of a power failure of more than 1 minute, sensors in the system will notify the control system, initiating a controlled shutdown of the system. The one minute allows minor fluctuations in the power to occur, such as momentary spikes, without shutting down the system.

Because of the requirement for high flexibility, the NI SCXI and AT-MIO-16E-10 products were selected for analog input and digital I/O interfacing with the furnace systems to the computer. For analog output interfacing, the NI AT-AO-10 board is used.

The software was designed with an intuitive graphical interface, giving users necessary information in an organized, understandable fashion. The actual systems are represented on- screen, with critical information located at their points of origin. This allows the user to immediately identify any problems and their location in the system due to failure or mis-programming. Then according to user access level, the user may manually change settings to correct the problems.

History and Data Logging are one of the biggest advantages to computer control systems. By monitoring all critical parameters, system and process control can be effectively maintained, minimizing manufacturing costs. The system at ISET has been set up to allow users to choose which data parameters to log. These parameters are currently stored on hard disk, but will soon be stored on CD for long term archival. The format of these files is readable by both MS Access and MS Excel for report generation. Using a database software, control charts are easily created from the accumulated data.

The current extent of control and monitoring is limited to the thermal processes. The flexibility and expandability of the current system will allow ISET to eventually control and monitor the other systems involved in the pilot line. This will primarily be executed in a distributed control scheme, with each system having its own local controller, monitored by the central CPU. The thermal processes may also become locally controlled by the

existing control system, which will then be monitored by a central CPU.

4.0 CONCLUSIONS AND FUTURE WORK

ISET has successfully developed and demonstrated a low cost, non-vacuum approach to grow solar cell grade CIS layers. At the present time, small area solar cells with over 12% efficiency can be fabricated using this novel technique. Repeatability of 9-10% efficient cells, on the average, is very good using pure CIS absorbers without any bandgap widening. A pilot line has been built during this research period to be able to process 1 ft^2 size modules and to identify problem areas associated with large area processing using the novel non-vacuum technique. Although total de-bugging of this line is not complete, experiments made so far indicate the following:

I) Stoichiometric uniformity of films over large areas is excellent. The nature of the process is such that we believe we can deposit films over much larger area substrates with uniform stoichiometry.

ii) Morphology of the films has been improved, however, there is still some porosity left in the layers. At the present time 9-12% efficiency can regularly be obtained for small area cells using CIS.

iii) Module integration is a topic that requires more development. The specific challenge associated with module integration arises from the fact that the films do not nucleate properly on the glass surface. As a result, CIS layers deposited on scribed MO substrates are discontinuous in the areas where the Mo layer is scribed and the glass surface is exposed. Unprotected edges of the Mo pads make contact with the top ZnO layer and cause deterioration of the fill factor.

We have processed small size submodules (10-30 cm^2) with conversion efficiencies of 6-8.2% using the non-vacuum technique. The future work will concentrate on the larger area 1 ft^2 size modules and a new module integration scheme that can avoid the problem listed above.

In terms of device efficiencies we believe that 12-13% efficiency that we have demonstrated is the maximum we can get with CIS and the present device structure. Work in Phase III will concentrate on taking this technology into larger areas, but at the same time inclusion of S in the films for bandgap widening.

Studies made on Na diffusion pointed out that this diffusion is a function of the nature of the Mo film as well as the nature of the CIS growth process. In fact comparing different CIS deposition processes we found that Na diffusion is more of a function of the film growth technique than anything else. we demonstrated that the non-vacuum technique can

achieve controlled Na doping and that there is an optimum level of doping that needs to be experimentally determined.

5.0 ACKNOWLEDGMENTS

Part of this work has been carried out under National CIS Partnership Program. The authors are grateful to the members of the "Mo/substrate interaction" working group which included J. Britt of EPV, T. Gillispie of Lockheed Martin, A. Rockett of University of Illinois, J. Sites of CSU, R. Matson, A. Swartzlander-Franz, S. Asher and M. Al-Jassim of NREL. We are also thankful to K. Emery of NREL for characterization and measurements of films and devices, and to H. Ullal, R. Noufi and K. Zweibel for extensive technical discussions.

6.0 LIST OF PUBLICATIONS

During the last 12 month period the following papers were published on the subject of thin film solar cells:

- B.M. Başol, V.K. Kapur, C.R. Leidholm, R. Roe, A. Halani and G. Norsworthy, "Low cost CIS device processing", NREL PV Program Rev. Meeting, Nov. 18-22, 1996, AIP Conf. Ser. 394, p.107.

- B.M. Başol, V.K. Kapur, A. Halani, C.R. Leidholm, J. Sharp, J. Sites, A. Swartzlander, R. Matson and H. Ullal, "CIGS Thin Films and Solar Cells Prepared by Selenization of Metallic Precursors", J. Vac. Sci. Technol. A., 14, 2251 (1996).

- B.M. Başol, V.K. Kapur, C.R. Leidholm, A. Halani and K. Gledhill, "Flexible and Light Weight CIS Solar Cells on Polyimide Substrates", Sol. Energy Matl. Sol. Cells, 43, 93 (1996).

- B.M. Başol, V.K. Kapur, C.R. Leidholm and A. Halani, "Flexible and Light Weight CIS Solar Cells", 25th IEEE PVSC, 1996, p.157.

7.0 REFERENCES

1. B.M. Basol et al., J. Vac. Sci. Technol. A, 14(4), July/Aug 1996, p. 2251.
2. B.M. Basol et al., First WCPEC, Dec. 5-9, 1994, Hawaii, p. 148

REPORT DOCUMENTATION PAGE

Form Approved
OMB NO. 0704-0188

1. AGENCY USE ONLY (Leave blank)	2. REPORT DATE	3. REPORT TYPE AND DATES COVERED
	August 1997	Annual Technical Progress Report,1 April 1996 - 31 March 1997

4. TITLE AND SUBTITLE

Application of CIS to High-Efficiency PV Module Fabrication, Annual Technical Progress Report, 1 April 1996 - 31 March 1997

5. FUNDING NUMBERS

C: ZAF-5-14142-07
TA: PV704401

6. AUTHOR(S)

B, Başol, V. Kapur, C. Leidholm, A. Halani, and G. Norsworthy

7. PERFORMING ORGANIZATION NAME(S) AND ADDRESS(ES)

International Solar Electric Technology (ISET)
8635 Aviation Blvd.
Inglewood, CA 90301

8. PERFORMING ORGANIZATION REPORT NUMBER

9. SPONSORING/MONITORING AGENCY NAME(S) AND ADDRESS(ES)

National Renewable Energy Laboratory
1617 Cole Blvd.
Golden, CO 80401-3393

10. SPONSORING/MONITORING AGENCY REPORT NUMBER

SR-520-23444

11. SUPPLEMENTARY NOTES

NREL Technical Monitor: H.S. Ullal

12a. DISTRIBUTION/AVAILABILITY STATEMENT

12b. DISTRIBUTION CODE

UC-1260

13. ABSTRACT *(Maximum 200 words)*

During this research period, International Solar Electric Technology (ISET) researchers concentrated their efforts on three different areas of research. Within the CIS Partnership Program, ISET participated in the "substrate/Mo interactions" working group and investigated issues such as Na diffusion from the soda-lime glass substrate into the Mo layers and CIS films. Researchers determined that the Na content within the Mo layers was not a strong function of the nature of the Mo film. However, diffusion through the Mo layers was found to be a function of the Mo film characteristics, as well as a very strong function of the CIS growth process. Na was found to be on the grain boundaries both in Mo and CIS layers. Much of the effort was spent on developing a low-cost, non-vacuum CIS deposition technique and on establishing a pilot facility to process approximately 1-ft^2 modules. The non-vacuum technique was successfully developed for CIS film growth. Layers prepared using this novel approach were used for solar cell and submodule fabrication. Small-area solar cells with total-area efficiencies of 12.4% were demonstrated. Submodules with efficiencies above 8% were also fabricated. The size of the submodules processed is currently limited to about 30 cm^2. 1-ft^2-size module processing will be initiated during the next phase of the program when the pilot line will be debugged and challenges faced in the integration process are remedied.

14. SUBJECT TERMS

photovoltaics ; copper indium diselenide ; CIS ; high-efficiency PV modules ; module fabrication

15. NUMBER OF PAGES
4 32

16. PRICE CODE

17. SECURITY CLASSIFICATION OF REPORT	18. SECURITY CLASSIFICATION OF THIS PAGE	19. SECURITY CLASSIFICATION OF ABSTRACT	20. LIMITATION OF ABSTRACT
Unclassified	Unclassified	Unclassified	UL